Journal of Alloys and Compounds 509 (2011) 5381–5387

Contents lists available at ScienceDirect

Journal of Alloys and Compounds

journal homepage: www.elsevier.com/locate/jallcom

Morphology-controlled synthesis of monodisperse silver spheres via a solvothermal method

Yashao Chen*, Yanlin Wei, Pengmei Chang, Linjing Ye

Key Laboratory of Applied Surface and Colloid Chemistry (Shaanxi Normal University), Ministry of Education, School of Chemistry and Materials Science, Xi'an 710062, People's Republic of China

ARTICLE INFO

Article history:
Received 6 August 2010
Received in revised form 9 February 2011
Accepted 9 February 2011
Available online 16 February 2011

Keywords:
Silver metal
Chemical synthesis
Nanostructures
Optical properties

ABSTRACT

Monodisperse silver spheres were successfully synthesized by a solvothermal method with the assistance of polyvinylpyrrolidone (PVP). The final products were characterized by X-ray diffraction (XRD), scanning electron microscopy (SEM), laser particle size analyzer, transmission electron microscopy (TEM), Fourier transform infrared spectrophotometer (FTIR), and UV–vis absorption spectroscopy. The as-synthesized silver spheres with cubic phase structure were nearly monodisperse and had an average diameter of 250 nm. The experimental results showed that their sizes and morphologies could be tailored by changing the reaction temperature, time, and PVP concentration under solvothermal conditions. The optical properties of silver spheres were investigated as a function of PVP concentration. A possible mechanism was presented for the formation of monodisperse silver spheres.

1. Introduction

During the last two decades, research on inorganic nanoparticles has been developing rapidly due to their exceptional electro-optical, magnetic and other physical and chemical properties. Among the noble metal nanoparticles, silver is perhaps the most widely recognized for its application in electronics [1], catalysis [2,3], bio-labeling [4,5], surface-enhanced Raman scattering (SERS), etc. [6–8]. Such properties and applications strongly depend on the morphologies and dimensions of the silver nanostructures. Therefore, the synthesis of silver nanoparticles with well-controlled morphology and a narrow particle size distribution is essential for uncovering their properties and achieving their practical applications.

So far, considerable attentions have been drawn to the preparation of silver nanoparticles with controlled shape and size [9–11]. To obtain these different-shaped nanomaterials, various techniques including physical and chemical approaches have been developed such as electrochemical [12,13], vapor-phase polymerization [14], laser ablation [15], UV-irradiated photoreduction [16,17], ultrasonic wave-assisted [18,19], wet-chemistry [20,21], biochemistry [22], chemical reduction–protection method [23–25], bionic technology [26,27] and so forth. Although nanocrystalline silver powders are well utilized in nanotechnology, challenges associated with a large-scale fabrication by a solution method are still formidable. Recently, PVP has been widely used in the synthesis of nanoparticles because both oxygen and nitrogen atoms of the pyrrolidone unit can facilitate PVP absorbed onto the surface of metal nanostructures, making it a good stabilizer for protecting the products from agglomeration [28–30]. However, the fabrication of silver nanospheres with well-controlled sizes in high yield, by a simple and low-cost route, remains a big challenge.

In this report, we propose a simple, low-cost and versatile method, PVP-assisted solvothermal route, to synthesize a large quantity of uniform silver spheres with controlled diameter. By changing the concentration of PVP, the size and morphology of the silver spheres could be readily controlled. A possible growth mechanism of the silver spheres is presented.

2. Experimental

2.1. Synthesis of silver spheres

In the present work, all the reagents were analytical grade and used without further purification. In a typical process, 42.5 mg PVP (K-30) was dissolved in 5 mL silver nitrate ($AgNO_3$, 0.05 M) solution under magnetic stirring at room temperature. The solution was then transferred into a 50 mL Teflon-lined stainless steel autoclave containing 20 mL polyethylene glycol (PEG-400), which was introduced as a reducing agent and solvent. The suspension was homogenized under vigorous stirring for 10 min. Subsequently, the autoclave was sealed, maintained at 120 °C for 6 h, and cooled down to room temperature rapidly. The precipitate was collected, washed with distilled water and ethanol several times, and dried in the vacuum drying oven at room temperature for 4 h.

* Corresponding author. Tel.: +86 29 85303725; fax: +86 29 85307774.
E-mail address: yschen@snnu.edu.cn (Y. Chen).

0925-8388/$ – see front matter © 2011 Elsevier B.V. All rights reserved.
doi:10.1016/j.jallcom.2011.02.054

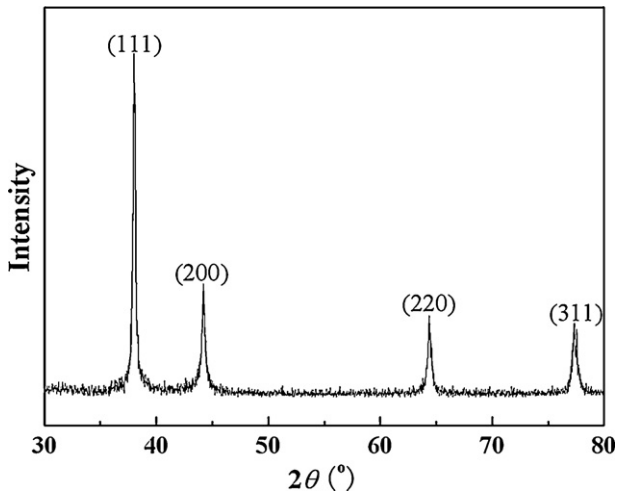

Fig. 1. XRD pattern of silver spheres synthesized at 120 °C for 6 h with 1.700 mg/mL PVP.

2.2. Characterization

The crystalline phase and structure of the as-synthesized products were identified by a D/Max2550VB+/PC X-ray diffractometer (Rigaku, Japan) with monochromated CuKα radiation (λ = 1.5418 Å) at 40 kV and 40 mA. The morphology, size and structural characteristics of the samples were examined using a Quanta 200 scanning electron microscope (FEI, The Netherlands) with an accelerating voltage of 20 kV and a JEM-3010 transmission electron microscope (JEOL, Japan) with an accelerating voltage of 300 kV, respectively. The particles size and their distribution were measured by BI-90Plus laser particle size analyzer (BIC, USA). The UV–vis absorption spectra were recorded on a Lambda 950 UV–visible spectrophotometer (Perkin-Elmer, USA). The Fourier transform infrared (FTIR) spectra of the samples were measured by a Nicolet Avatar 360 spectrophotometer (Thermo Nicolet, USA).

3. Results and discussion

The crystal structure of the samples synthesized at 120 °C for 6 h with 1.700 mg/mL PVP were confirmed by XRD. As shown in Fig. 1, all the diffraction peaks can be readily indexed to the cubic phase of Ag (JCPDS card No. 04-0783), belonging to the Fm3 m space group. The peaks at 38.1°, 44.3°, 64.4° and 77.8° are well corresponded as (1 1 1), (2 0 0), (2 2 0) and (3 1 1) planes of face-centered-cubic (fcc) silver with a lattice constant of a = 4.080 Å, which is consistent with the previously reported data (a = 4.086 Å). From the strong and sharp diffraction peaks in the XRD pattern, it can be concluded that the as-obtained samples are well crystalline.

Fig. 2 displays the selected area electron diffraction (SAED) pattern and high-resolution transmission electron microscopy (HRTEM) image of the samples synthesized at 120 °C for 6 h with 1.700 mg/mL PVP. In Fig. 2a, the SAED pattern was obtained by directing the electron beam perpendicular to the surface of silver sphere. The SAED pattern presenting hexagonal symmetry diffraction spots confirms that the sphere is well crystalline, which means that the as-synthesized silver spheres are perfect single crystals. The HRTEM image, shown in Fig. 2b, provides further insights into the crystal structure of the as-prepared silver spheres. Some fringes of crystallographic planes are observed but they are not well defined.

To study the mechanism for formation of silver spheres prepared by a simple solvothermal process, the samples synthesized at 120 °C for 1.700 mg/mL PVP with different reaction times (0.5, 3, 6, 9, and 24 h) are systematic investigated. The SEM, TEM, and HRTEM images of the samples are shown in Fig. 3 as a function of reaction time. Some of these images clearly show the agglomeration of spherical silver particles. As shown in Fig. 3a and Fig. 3b, silver nanocrystals with the size of 10–20 nm are formed in the solution system after 30 min of initial reaction, and some particles possess spherical shape. When the reaction time is increased to 3 h, the aggregated particles with irregular shape are formed (Fig. 3c). By prolonging the reaction time to 6 h, a large quantity of silver spheres with diameters in the range of 200–300 nm are formed (Fig. 3d); it also shows nearly perfect spherical silver particles without any aggregation. As the reaction time is extended to 9 h, the diameter of silver spheres is increased to about 800 nm; apparently, some irregular particles are also present (Fig. 3e). When the reaction time is further increased to 24 h, the average size of the silver spheres has a slight change compared to that of the samples prepared for 9 h; however, a number of irregular particles are formed along with silver spheres (Fig. 3f). The sizes of silver spheres are becoming larger with an increase in reaction time, and small silver spheres are slowly dissolved into the solution and recrystallized on the larger ones. This process can probably be attributed to the involvement of Ostwald ripening in the crystal growth [31].

The synthesis temperature also plays an important role in structure change of silver spheres at various stages of the growth process. By simply changing the reaction temperature, the size and shape can be significantly tuned. The products are dominated by silver spheres at a temperature from 90 °C to 150 °C. In contrast, when temperatures ≥150 °C it was not beneficial for the formation of silver spheres. The SEM images of silver particles prepared at different temperatures for 6 h with 1.700 mg/mL PVP are shown in Fig. 4. As can be seen in Fig. 4a, the resultant products synthesized at 90 °C are densely agglutinated and have a small size distribution in the range of 50–100 nm. Compared to that of the sample prepared at 90 °C, the sample having very few irregular particles is

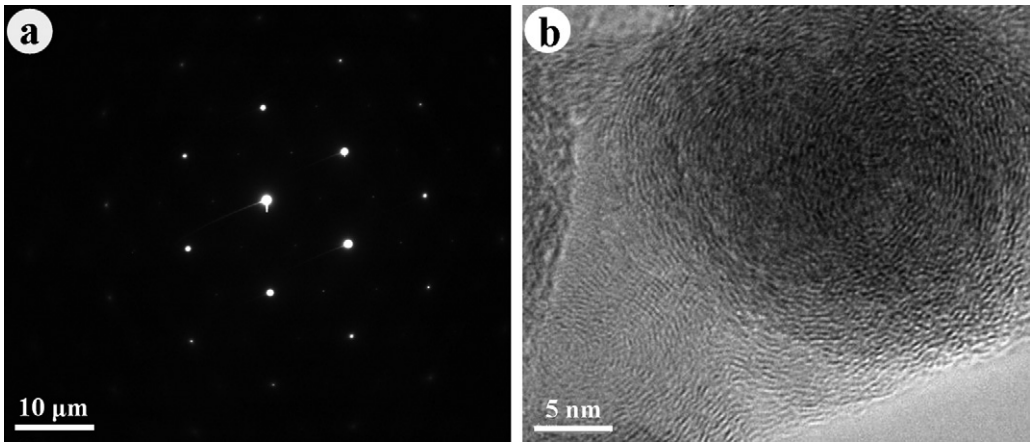

Fig. 2. SAED pattern (a) and HRTEM image (b) of silver spheres synthesized at 120 °C for 6 h with 1.700 mg/mL PVP.

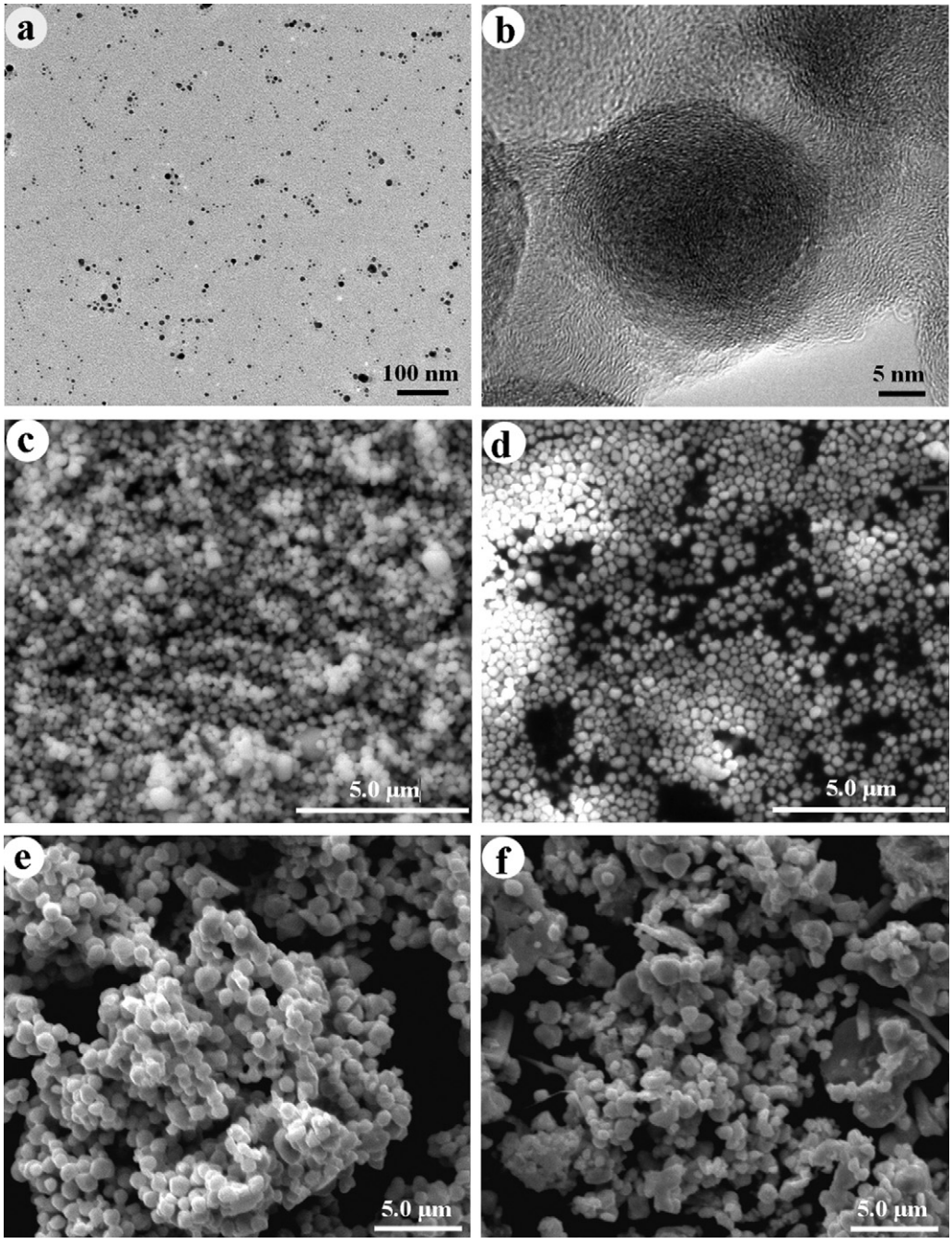

Fig. 3. TEM and SEM images of silver spheres synthesized at 120 °C with 1.700 mg/mL PVP for different reaction times: (a and b) 0.5 h; (c) 3 h; (d) 6 h; (e) 9 h; (f) 24 h.

mainly composed of spheres when the reaction temperature is set to 120 °C. This indicates that the as-prepared nanoparticles have spherical shape with an average diameter of 250 nm, as shown in Fig. 4b. At 150 °C, the products are dominantly composed of irregular silver particles instead of regular silver spheres. When the reaction temperature is further increased to 180 °C, the products are mainly composed of quasi-spherical (including some sharp or truncated corners) silver nanoparticles. These nanoparticles have a wider size distribution from 100 nm to 1000 nm, as illustrated in Fig. 4d.

Although PVP has been widely used as a reducing agent, it probably acts as a capping agent in PEG solution. In the absence of PVP, we could also obtain silver nanoparticles. However, without the capping agent, the size and shape will be not uniform. This also confirms that the PEG-400 played roles as reducing reagent. In order to optimize the fabrication of well-controlled silver spheres, a more detailed investigation of silver particles prepared with different PVP concentrations was carried out by SEM (Fig. 5). When PVP with the concentration of 1.700 mg/mL is introduced into the reaction system, a large quantity and good uniformity of silver spheres are achieved, as shown in Fig. 5e. The product consisting of well-defined silver spheres with an average diameter of 250 nm and a narrow particle size distribution of 230 nm to 280 nm are obtained (Fig. 5f). In contrast, when the PVP concentration is decreased to 0.085 mg/mL, it can be clearly seen that the resultant products are aggregated nanoparticles. Smaller spheres with an average diameter of 150 nm and a narrow particle size distribution of 120–180 nm are obtained (Fig. 5a and b). With 1.132 mg/mL PVP, the as-prepared

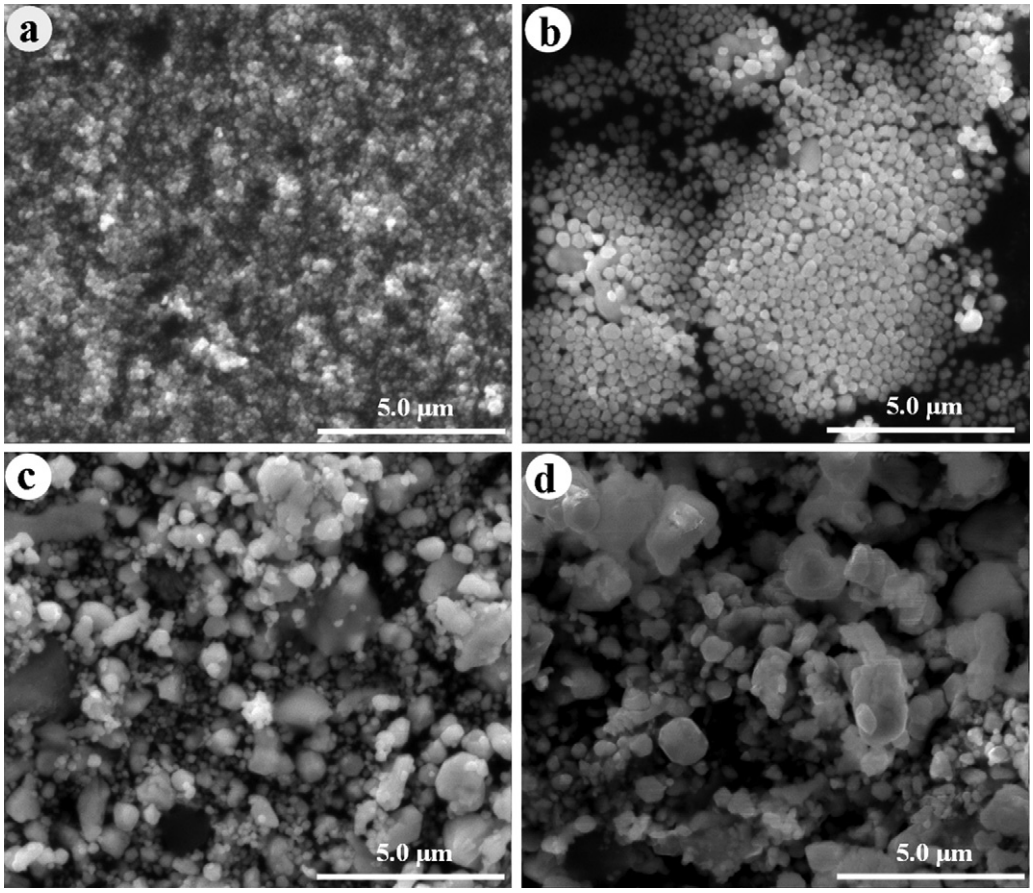

Fig. 4. SEM images of silver spheres synthesized at different temperatures with 1.700 mg/mL PVP for 6 h: (a) 90 °C; (b) 120 °C; (c) 150 °C; (d) 180 °C.

products are composed of spheres and some irregular nanoparticles with a wider particle size distribution ranging from 100 nm to 600 nm, as presented in Fig. 5c and d. When the PVP concentration is increased to 3.400 mg/mL, the diameter of silver spheres is increased to 500–600 nm. Interestingly, some spheres are closely linked and fused into each other (Fig. 5g and h). It can be seen that the average particle diameter is increased and the lognormal size distribution is narrowed as the PVP concentration increases. One reason is that with PVP concentration increasing, the polymer chain of PVP molecule in an entangled network may take place, so that the wrapped silver particles coalescence to form a relatively larger average size. Another reason is that, at relatively high temperatures, capping agent may be desorption from the nucleus due to the heating [32], which lead to Ostwald ripening phenomenon. So even if with a very high PVP concentration, large particles can also be generated by temperature. The corresponding XRD patterns of the samples prepared at 120 °C for 6 h are shown in Fig. 6 as a function of the PVP concentration. All the diffraction peaks indicate that the as-prepared samples are phase-pure silver with a hexagonal structure. It is apparent that the diffraction peaks become narrower and sharper with an increase in PVP concentration, indicating the growth of the silver nanocrystallites.

In order to study the effects of particle morphology on the optical properties, the samples synthesized at 120 °C for 6 h with different PVP concentrations were further investigated by UV–vis spectroscopy. As shown in Fig. 7a, the silver spheres prepared with 0.085 mg/mL PVP exhibit an extinction peak at 410 nm with a narrow full width. The extinction peak of silver spheres prepared with 1.132 mg/mL PVP is around 430 nm (Fig. 7b), which has a 20 nm red-shift. It is much wider in comparison to that of the samples prepared with 0.085 mg/mL PVP. When the PVP concentration is increased to 1.700 mg/mL, the extinction peak is slightly blue-shift to 425 nm (Fig. 7c) with a narrow full width at half-maximum, which is in accordance with the SEM result (Fig. 5e and f). When the PVP concentration is 3.400 mg/mL, the extinction peak is red-shift to 445 nm (Fig. 7d), and the extinction band is much broader due to the larger size and wider particle size distribution of the silver spheres. These results are consistent with the SEM results (Fig. 5g and h).

To further investigate the interaction between PVP molecules and silver spheres, TEM and FTIR were conducted. Fig. 8 displays a TEM image of silver sphere with an average diameter of 250 nm. It is shown that the small black silver nanoparticle is located on the centre of sphere, which has a layer of an imaginary polymer on its surface. This image clearly shows that the PVP is simultaneously adsorbed on the surface of silver spheres during the evolution of small silver nanoparticles. FTIR spectra are another evidence for the coverage of the PVP on the silver spheres. Fig. 9 shows the main features of pure PVP and the prepared silver spheres with 1.700 mg/mL PVP. It can be seen that both samples have the very similar spectra. Compared with that of the pure PVP, the appearance of stretching vibrations at 1126 cm^{-1} confirms that maybe the PVP molecule is coordinated to the silver surface through the nonbonding electrons of the oxygen atom in carbonyl. At the same time, the significant signals at 2942 cm^{-1} and 2850 cm^{-1}, asymmetric stretching vibration of CH_2 in the skeletal chain of PVP, reveals that the CH_2 chain is close to the surface of silver spheres. This evidences that PVP is adsorbed on the silver nanoparticles surface during the crystal growth process.

In order to identify the reduction role of PEG-400 in the formation of silver nanoparticles, the products obtained in the absence of PEG-400 were characterized by XRD, as shown in Fig. 10. Only

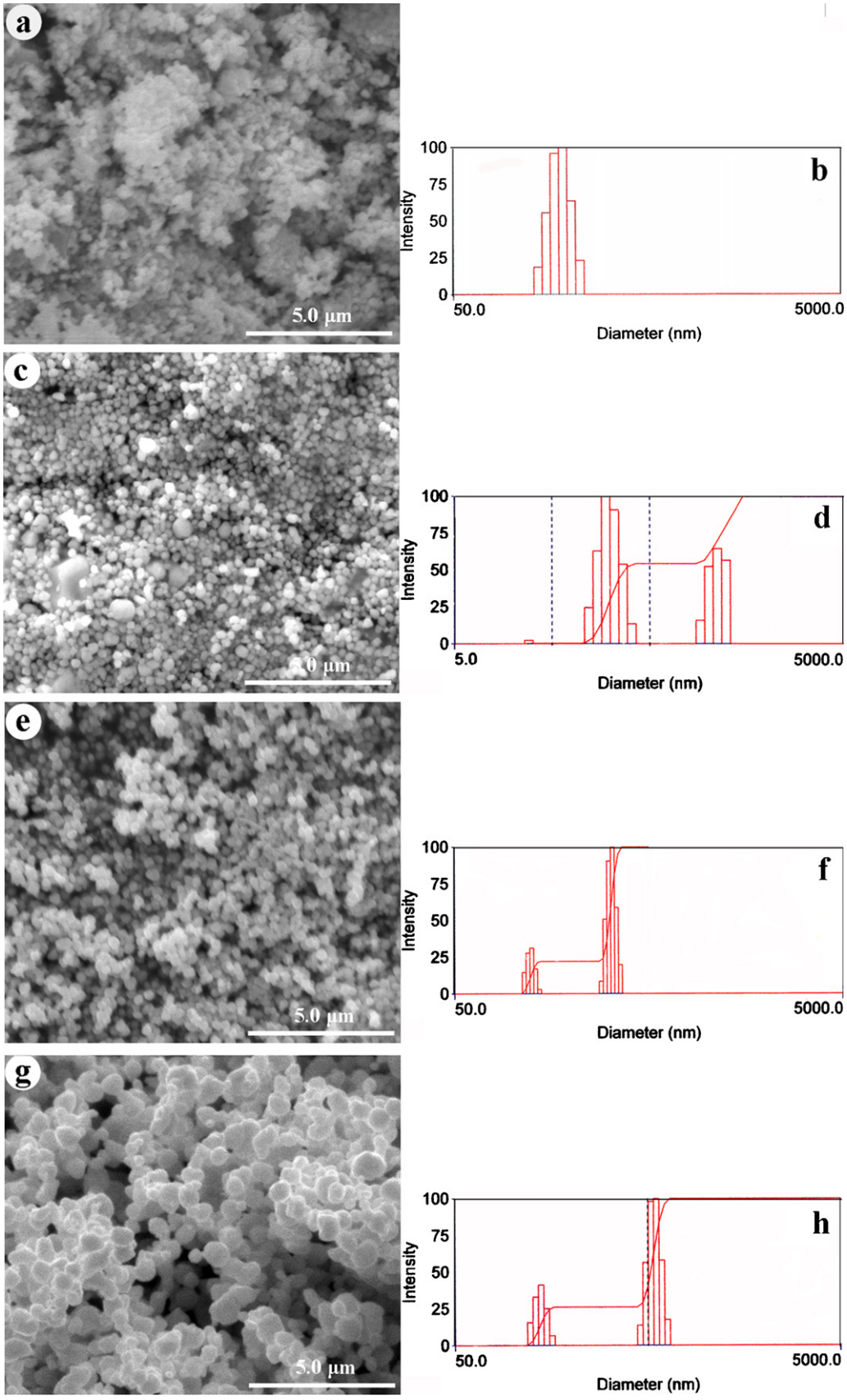

Fig. 5. SEM images and particle size distribution of silver spheres synthesized at 120 °C for different PVP concentrations (m_{PVP}:$V_{solution}$): (a and b) 0.085 mg/mL; (c and d) 1.132 mg/mL; (e and f) 1.700 mg/mL; (g and h) 3.400 mg/mL.

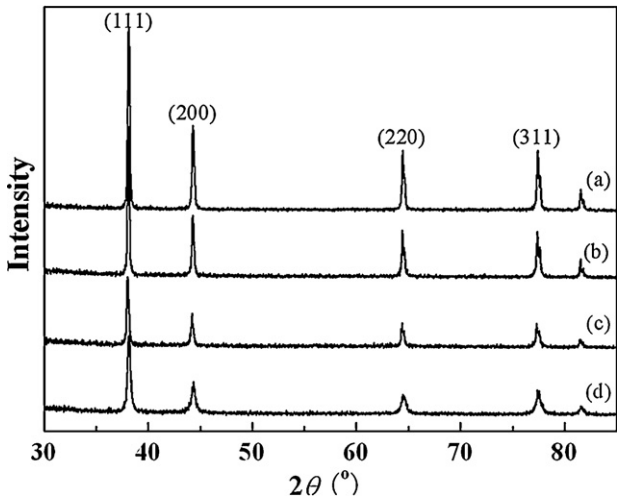

Fig. 6. XRD patterns of silver spheres synthesized at 120 °C for different PVP concentrations (m_{PVP}:$V_{solution}$): (a) 0.085 mg/mL; (b) 1.132 mg/mL; (c) 1.700 mg/mL; (d) 3.400 mg/mL.

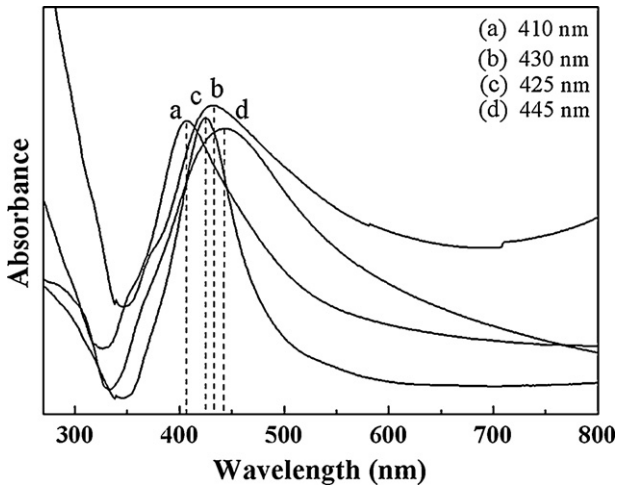

Fig. 7. UV–vis absorption spectra of silver spheres synthesized at 120 °C for different PVP concentrations (m_{PVP}:$V_{solution}$): (a) 0.085 mg/mL; (b) 1.132 mg/mL; (c) 1.700 mg/mL; (d) 3.400 mg/mL.

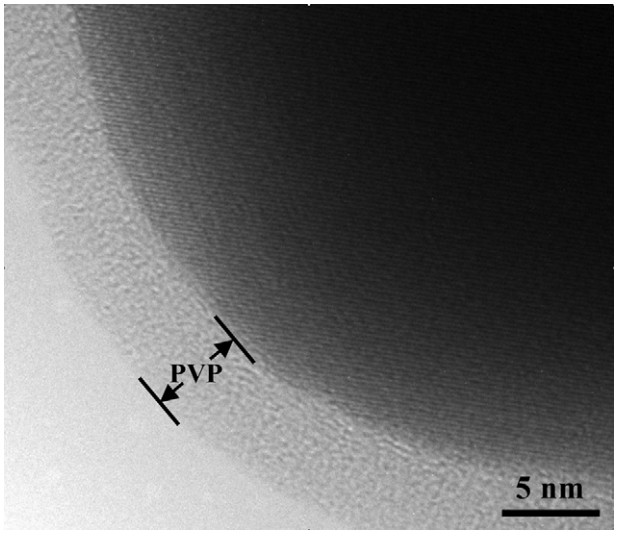

Fig. 8. TEM image of silver spheres synthesized at 120 °C for 6 h with 1.700 mg/mL PVP.

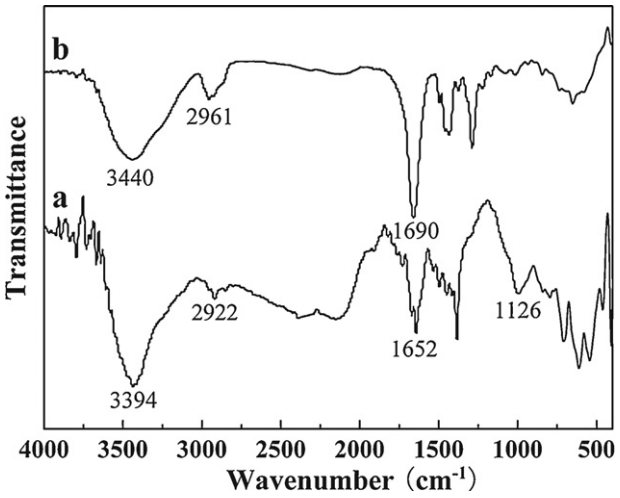

Fig. 9. FTIR spectra of silver spheres synthesized at 120 °C for 6 h with (a) 1.700 mg/mL PVP and (b) pure PVP.

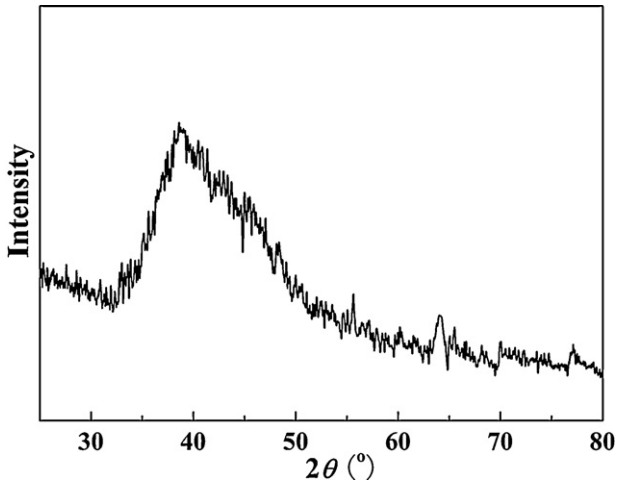

Fig. 10. XRD pattern of the silver spheres obtained at 120 °C for 6 h in the absence of PEG-400.

a weak and broad diffraction peak at 38.0° is observed, indicating the formation of silver particles with poor crystalline quality. This confirms that the PEG-400 has a stronger reduction than PVP in the formation of silver nanoparticles.

Based on the above results, a possible mechanism for the formation of silver spheres is tentatively proposed. In our experiment, the growth of silver spheres involves a multistep process: in an initial stage, single-crystal seeds and twinned seeds can be formed through the homogeneous nucleation, as shown Fig. 11. In the initial stage (step A), silver atoms generated from the reduction of $AgNO_3$ diffuse to the surface of nuclei and position themselves at active surface sites, forming metallic bonds with their neighbors. As thermodynamic growth occurs there is physical adsorption of the diffusing nanoparticles once they are in contact with one another (step B). The PVP forms just a very weak interaction especially with the isotropic nanoparticles, which influence the gradual growth of silver nanoparticles. In the subsequent growth process (step C), by adjusting the molar ratio between PVP and $AgNO_3$, the thickness of PVP coating and the location of PVP chains on the surface of a seed could both be modified. This modification, in turn, alters the resistance of each facet to growth (addition of silver atoms), and led to the formation of silver nanostructures with distinct shapes. In the later case (step D), the selectivity in interaction between PVP and various crystallographic planes is lost because such loss enables a

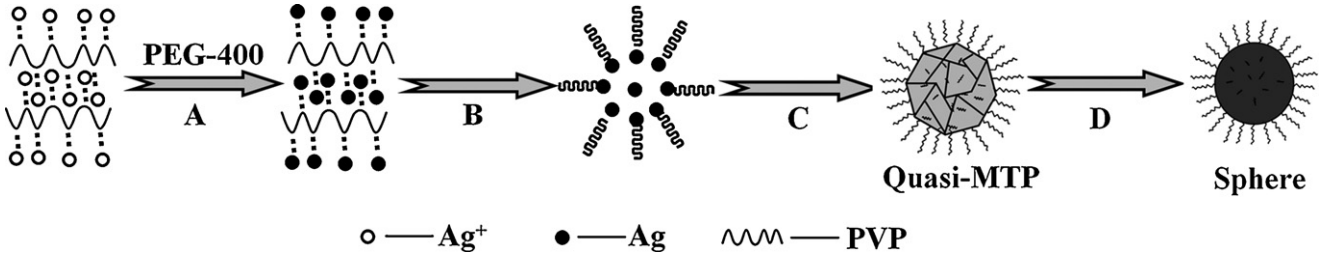

Fig. 11. Schematic illustration of the mechanism proposed to account for the growth of silver spheres. (A) The reduction of silver ions by PEG-400; (B) the formation of clusters; (C) the growth of seeds with assistance of PVP; (D) the evolution of spheres from a multiply twinned particle of silver.

lower surface energy, thus inducing no anisotropic growth. From the experimental results, it can be concluded that the concentration of PVP seems to be an important factor in kinetically controlling the nucleation and growth of silver spheres. Both oxygen and nitrogen atoms of the pyrrolidone unit can facilitate PVP adsorbed onto the surface of metal nanostructures, making PVP a good stabilizer to protect the product from agglomeration.

4. Conclusions

In summary, monodisperse silver spheres in high yields have been successfully prepared by solvothermal process. PEG and PVP were employed as a reducing agent and capping agent, respectively. The present method is advanced in its simplicity, high yield and controllability. Uniform silver spheres with an average diameter of 250 nm could be routinely synthesized at 120 °C for 6 h with 1.700 mg/mL PVP. The morphology and dimensions of the silver spheres are highly dependent on PVP concentration, the synthesis reaction time and temperature. Among these factors, the PVP concentration has the strongest effect on silver spheres morphology. It is expected that reduction of metal salts by the end groups of a polymer may eventually provide an environmentally benign and scalable route to morphology-controlled synthesis of metal nanocrystals. We believe that this new strategy is applicable to other noble metals and organic polymers.

Acknowledgements

We would like to thank Mr. Chen Dichun from Xi'an University of Technology for his helps in TEM analysis. This work was fully supported by the grant from the Science and Technology Research Project of Xi'an City (CXY09026)

References

[1] D.D. Evanoff, G. Chumanov, J. Phys. Chem. B 108 (2004) 13948–13956.
[2] K. Mallick, M. Witcomb, M. Scurrell, Mater. Chem. Phys. 97 (2006) 283–287.
[3] A.E. Sanli, I. Kayacan, B.Z. Uysal, M.L. Aksu, J. Power Sources 195 (2010) 2604–2607.
[4] A.D. McFarland, R.P. Van Duyne, Nano Lett. 3 (2003) 1057–1062.
[5] J. Zhang, J. Malicka, I. Gryczynski, J.R. Lakowicz, J. Phys. Chem. B 109 (2005) 7643–7648.
[6] P.L. Stiles, J.A. Dieringer, N.C. Shah, R.P. Van Duyne, Annu. Rev. Anal. Chem. 1 (2008) 601–626.
[7] M.J. Banholzer, J.E. Millstone, L.D. Qin, C.A. Mirkin, Chem. Soc. Rev. 37 (2008) 885–897.
[8] W.Y. Li, P.H.C. Camargo, X.M. Lu, Y.N. Xia, Nano Lett. 9 (2009) 485–490.
[9] Y.N. Xia, Y.J. Xiong, B.K. Lim, S.E. Skrabalak, Angew. Chem. Int. Ed. 48 (2009) 60–103.
[10] Y. Qin, Y. Song, N.J. Sun, N.N. Zhao, M.X. Li, L.M. Qi, Chem. Mater. 20 (2008) 3965–3972.
[11] J.Y. Chen, B.J. Wiley, Y.N. Xia, Langmuir 23 (2007) 4120–4129.
[12] H.J. Chen, F. Simon, A. Eychmller, J. Phys. Chem. C 114 (2010) 4495–4501.
[13] C.D. Gu, T.Y. Zhang, Langmuir 24 (2008) 12010–12016.
[14] P. Mohanty, I. Yoon, T. Kang, K. Seo, K.S.K. Varadwaj, W. Choi, Q. Park, J.P. Ahn, Y.D. Suh, H. Ihee, B. Kim, J. Am. Chem. Soc. 129 (2007) 9576–9577.
[15] M. Darroudi, M.B. Ahmad, R. Zamiri, A.H. Abdullah, N.A. Ibrahim, K. Shameli, M.S. Husin, J. Alloys Compd. 509 (2011) 1301–1304.
[16] M.S. Chargot, A. Gruszecka, A. Smolira, K. Bederski, K. Głuch, J. Cytawa, L. Michalak, J. Alloys Compd. 486 (2009) 66–69.
[17] M. Darroudi, M.B. Ahmad, K. Shameli, A.H. Abdullah, N.A. Ibrahim, Solid State Sci. 11 (2009) 1621–1624.
[18] H.J. Chen, E. Kern, C. Ziegler, A. Eychmüller, J. Phys. Chem. C 113 (2009) 19258–19262.
[19] I.A. Wani, A. Ganguly, J. Ahmed, T. Ahmad, Mater. Lett. 65 (2011) 520–522.
[20] R.C. Jin, Y.C. Cao, E. Hao, G.S. Métraux, G.C. Schatz, C.A. Mirkin, Nature 425 (2003) 487–490.
[21] R. Shankar, B.B. Wu, T.P. Bigioni, J. Phys. Chem. C 114 (2010) 15916–15923.
[22] A.R. Shahverdi, S. Minaeian, H.R. Shahverdi, H. Jamalifar, A.A. Nohi, Pro. Biochem. 42 (2007) 919–923.
[23] J.G. Liu, X.Y. Li, X.Y. Zeng, J. Alloys Compd. 494 (2010) 84–87.
[24] D. Li, B.Y. Hong, W.J. Fang, Y.S. Guo, R.S. Lin, Ind. Eng. Chem. Res. 49 (2010) 1697–1702.
[25] P.S. Mdluli, N. Revaprasadu, J. Alloys Compd. 469 (2009) 519–522.
[26] V.K. Shukla, R.P. Singh, A.C. Pandey, J. Alloys Compd. 507 (2010) L13–L16.
[27] E. Bulut, M. Özacar, Ind. Eng. Chem. Res. 48 (2009) 5686–5690.
[28] J.M. McLellan, Y.J. Xiong, M. Hu, Y.N. Xia, Chem. Phys. Lett. 417 (2006) 230–234.
[29] Y.Y. Li, J.P. Liu, X.T. Huang, G.Y. Li, Cryst. Growth Des. 7 (2007) 1350–1355.
[30] A.S. Grijalva, R.H. Urbina, J.F.R. Silva, M.Á. Borja, F.F.C. Barraza, A.P. Amarillas, Mater. Res. Bull. 43 (2008) 90–96.
[31] A.R. Roosen, W.C. Carter, Physica A 261 (1998) 232–247.
[32] A.S. Barnard, X.M. Lin, L.A. Curtiss, J. Phys. Chem. B 109 (2005) 24465–24472.